Photocatalytic Hydromethylation and Hydroalkylation of Olefins Enabled by Titanium Dioxide Mediated Decarboxylation

Qilei Zhu and Daniel G. Nocera*

ABSTRACT: A versatile method for the hydromethylation and hydroalkylation of alkenes at room temperature is achieved by using the photooxidative redox capacity of the valence band of anatase titanium dioxide (TiO_2). Mechanistic studies support a radical-based mechanism involving the photoexcitation of TiO_2 with 390-nm light in the presence of acetic acid and other carboxylic acids to generate methyl and alkyl radicals, respectively, without the need for stoichiometric base. This protocol is accepting of a broad scope of alkene and carboxylic acids, including challenging ones that produce highly reactive primary alkyl radicals and those containing functional groups that are susceptible to nucleophilic substitution such as alkyl halides. This methodology highlights the utility of using heterogeneous semiconductor photocatalysts such as TiO_2 for promoting challenging organic syntheses that rely on highly reactive intermediates.

Photoredox catalysis has significantly expanded the methods available for radical-based carbon-carbon and carbon-heteroatom bond formation.[1–6] Owing to the increased driving force afforded by excited states, photoredox methods are especially valuable for generating highly reactive intermediates such as alkyl radicals. Strategies for facile alkyl radical generation, such as decarboxylation, often rely on adjacent substituents (e.g., arenes, heteroatoms and alkyl chains) to stabilize the resultant radical center.[7] Such an approach is not viable for the generation of methyl radicals (Me•), which are difficult to generate owing to sluggish C–C bond cleavage kinetics[8,9] together with unfavorable thermodynamics.[10,11] Thus, ingenious strategies are required for methylation such as the elegant cascade protocol developed for radical hydromethylation of olefins and C–H methylation of arenes,[12,13] though multi-step sequences and super stoichiometric reagents are required. Alternatively, heterogeneous photocatalysts,[14–17,18–21] and particularly semiconducting photoabsorbers, possess photoredox properties that are amenable for the generation of alkyl and specifically methyl radicals. Significant oxidizing power may be associated with hole equivalents in the valence band (VB) of semiconductors (Figure 1).[22,23] For example, the deep valence band (2.7 V vs. NHE) and wide band gap (3.2 eV) of anatase TiO_2 presages it as a particularly useful photocatalyst for oxidative decarboxylation. Indeed, photolyzed TiO_2 has been used to produce stabilized secondary and tertiary alkyl radicals for alkylation and annulation reactions[24] but this strategy was unsuccessful for the incorporation of primary alkyl radicals including Me•.[25] Nonetheless, the photo-oxidative degradation of acetic acid to produce Me• has been observed on single-crystal surfaces of TiO_2[26] and it is known that the decarboxylation of acetic acid by TiO_2 occurs prevalently in aerobic oxidation and pollutant-degradation conversion processes,[27,28] that rely on the production of Me• as an intermediate. Moreover, carboxylic acids, including acetic acid, are known to associate to the surface of TiO_2.[29] Accordingly, TiO_2 may promote redox-induced decarboxylation via inner-sphere electron transfer (ET), thus lowering the kinetic barrier for the generation of reactive intermediates. Harnessing the methyl radical from the decarboxylation of acetic acid on TiO_2 presents a powerful potential synthetic strategy for photoredox methods. We now report the facile photocatalytic hydromethylation and hydroalkylation reaction of alkenes via the decarboxylation of acetic acid and a variety of other acids, respectively, mediated by photoexcited anatase TiO_2 (Scheme 1). The method is particularly attractive as the reaction occurs with the use of free carboxylic acids under mildly acidic conditions

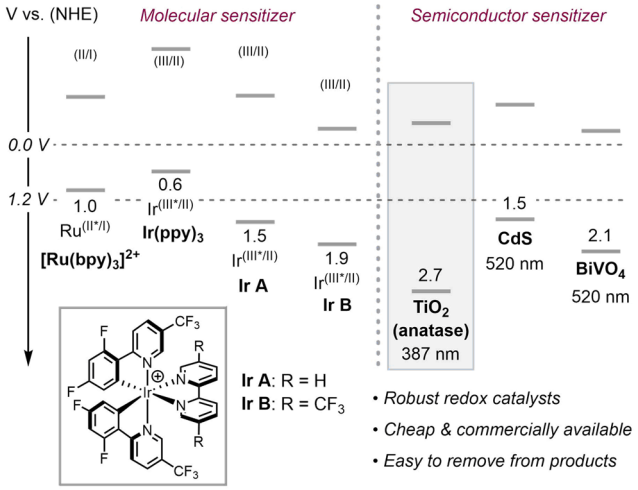

Figure 1. Redox potentials of selected molecular photocatalysts and band energy levels of several semiconductor photocatalysts.

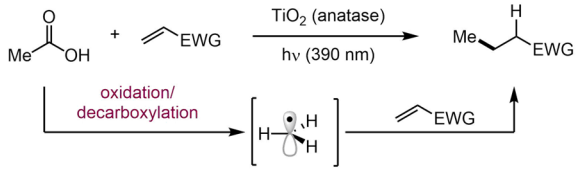

Scheme1. TiO_2-mediated hydromethylation of olefins enabled by decarboxylation of acetic acid.

Table 1. Survey of a hydromethylation reaction with various heterogeneous semiconducting photocatalysts.

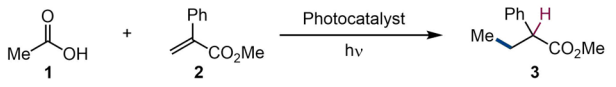

Entry[a]	Photocatalyst (λ_{irr})	Solvent	Yield (%)
1	TiO_2 (390 nm)	MeCN	86
2	ZnO (390 nm)	MeCN	7
3	WO_3 (440 nm)	MeCN	0
4	Carbon nitride (440 nm)	MeCN	0
5	$BiVO_4$ (white light)	MeCN	0
6	CdS (white light)	MeCN	0
7	TiO_2 (390 nm)	PhCN	85
8	TiO_2 (390 nm)	CH_2Cl_2	37
9	TiO_2 (390 nm)	PhF	60
Entry[a]	**Changes from entry 1**		**Yield (%)**
10	No TiO_2 catalyst		0
11	No irradiation		0
12	1.0 eq. $TiCl_4$ instead of TiO_2 catalyst		0
13	1.0 eq. $Ti(O^iPr)_4$ instead of TiO_2 catalyst		4

[a] Reactions were run on 0.1 mmol scale and the yields are determined by GC analysis relative to an internal standard.

without the need for stoichiometric base, which is required for typical decarboxylation strategies governed by outer sphere ET.[7] Accordingly, the photoredox method reported herein circumvents byproducts from base and carboxylate anion induced halide elimination and nucleophilic substitution reactions, thus increasing the scope and improving the atom economy of carbon-carbon bond formation of synthetic methyl/alkylation methods.

The heterogeneous semiconductors listed in Table 1 (entries 1–6) were surveyed as photocatalysts for the reaction between acetic acid and Michael acceptor **2**; excitation wavelengths were chosen to match the band gap of a given semiconductor. Conversion to product **3** depends on the oxidizing power of the VB of the semiconductor excepting ZnO, which is unstable in acidic conditions. Anatase TiO_2 photocatalyzes the desired transformation of **2** and acetic acid to **3** with a GC yield of 86% in the presence of only three equivalents of acetic acid. Optimization of the TiO_2 catalyst and acetic acid loadings is included in Tables S1 and S2. All reactions were run in disposable commercial borosilicate glass vials for which the 390-nm excitation wavelength of the LEDs lies outside the UV cutoff of borosilicate glass. Better yields were obtained for reactions performed in in polar solvents (entry 7–9), possibly due to facilitated ET between TiO_2 and acetate in polar media. Control experiments (entry 10–11) demonstrate that light irradiation and TiO_2 catalysts are essential for the desired reactivity. Furthermore, to examine whether solubilized Ti(IV) is responsible for the transformation, the TiO_2 nanopowder catalyst was replaced with stoichiometric amounts of $TiCl_4$ and $Ti(O^iPr)_4$. The reactions were drastically inhibited (entries 12 and 13), indicating the critical role of heterogeneous TiO_2 nanoparticles in promoting the methylation reaction of the olefin.

The substrate scope for the TiO_2 photoredox methyl-/alkylation reactions is summarized in Table 2. Synthetic procedures and characterization of substrates and products are described in Supporting Information. Alkene **2** produces the desired product **3** with an 84% isolated yield. For α-arylacrylates, various substituents are tolerated under the standard conditions (Methods B-D, see Supporting Information), including electron-withdrawing (**4**–**7**) and -donating (**8**–**10**) groups, as well as naphthyl (**11**) and pyridyl (**12**) derivatives. Besides arylacrylates, aryl-substituted enone (**13**), acrylonitrile (**14**) and acrylamide (**15**) also yield the desired hydromethylation products with high yields. Moreover, we found that alkenes undergo conversion without arene substituents. For example, fumarate, maleate (**16**), cyclohexanone (**17**), methacrylate (**18**) and vinylsulfone (**19**) can be hydromethylated smoothly. Tri-substituted alkenes (**20**–**22**) successfully afforded the desired products in moderate yields. Nominally, the quaternary carbon-centered product was produced from the tetrasubstituted alkene **23**, albeit with low efficiency. Surprisingly, 2- and 4-vinyl pyridines (**24** and **25**), which lack the carbonyl-derived electron withdrawing group (EWG), converted to the hydromethylated product with 85% and 84% yields, respectively. However, initial trials with styrene under standard conditions yielded no product. This observation is consistent with the SOMO orbital of styryl radical ($\boldsymbol{E}(PhCHCH_3^{\bullet/-})$ = −1.25 V vs. NHE)[30] lying to higher energy than the conduction band (CB) of TiO_2, thus preventing reduction of the styryl radical to the carbanion, which may subsequently be protonated to yield product. Inspired by the recent development of synergistic incorporation of hydrogen atom transfer (HAT) co-catalysts in photoredox catalysis,[31–33] hydromethylation products were observed with styrene derivatives (**26**, **27**) in the presence of a thiol-based HAT co-catalyst (see Supporting Information), for which the reaction conditions remain to be optimized.

We next examined the scope of the TiO_2-photoredox alkylation reaction with different carboxylic acid sources. The standard photoreaction conditions used for methylation were maintained. Primary (**28**, **29**), secondary (**30**, **31**), tertiary (**32**), benzylic (**33**) and homobenzylic (**34**) carboxylic acids are effective coupling partners. Ostensibly, the carbocyclic ring of cyclopropane and cyclobutane-derived carboxylic acids (**35**, **36**) can also be tolerated. Similarly, carboxylic acids bearing α-heteroatom substituents, e.g. alkyl ether (**37**, **38**), aromatic ether (**39**), ester (**40**), thioether (**41**), and amide (**42**), afforded the desired products in high yields without over-oxidation. An advantage of heterogeneous photocatalysts is their superior stability as compared to molecular photocatalysts, which are vulnerable to attack by free radicals, especially for less hindered and localized primary carbon radicals.[34, 35] In this regard, substrates with nascent functional group reactivity derived from primary carboxylic acids were explored. The TiO_2 photoredox method was tolerant to sulfonamide (**43**), ester (**44**), carboxylic acid (**45**), and ketone (**46, 47**) groups. Though intramolecular cyclization of a carbon-centered radical with unsaturated moieties is well-established, [36, 37] the method also tolerated carboxylic acids bearing alkene (**48**, **49**) and alkyne (**50**) motifs, which converted to products smoothly under standard conditions, suggesting facile intermolecular radical addition of the primary carbon-centered radical intermediate. Moreover, in contrast to outer-sphere electron transfer mediated oxidation of carboxylate anion, free carboxylic acids, which are less nucleophilic than the corresponding deprotonated anion, can be directly used here as an alkylation reagent without the need for an ancillary base, thus circumventing the production of nucleophilic substitution/ cyclization byproducts. For example, halogen-substituted carboxylic acid substrates afforded the desired hydroalkylation products in moderate to high

Table 2. Scope of olefins and carboxylic acids for TiO_2 photoredox methylation and alkylation.

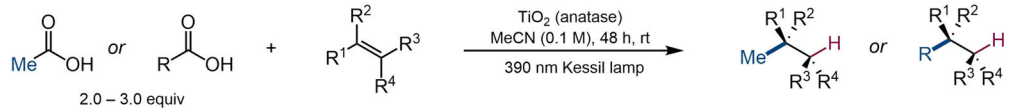

Alkene scope

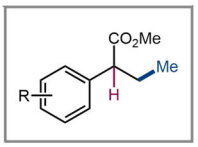

3 R = H, 84%
4 R = 4-F, 63%
5 R = 4-Cl, 67%
6 R = 3-Br, 83%
7 R = 4-Br, 81%
8 R = 3-OMe, 64%
9 R = 4-OMe, 44%
10 R = 2-Me, 73%

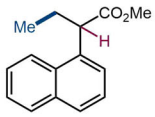

11 83%

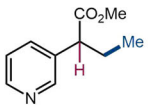

12 78%

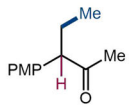

PMP = 4-MeOC$_6$H$_4$
13 74%

14 87%

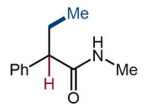

15 73%

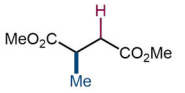

16 57%[a] (from *E*-olefin)
56%[a] (from *Z*-olefin)

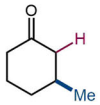

17 43%[a]

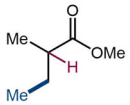

18 53%[a]

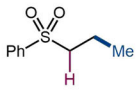

19 54%

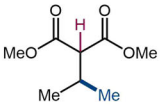

20 53%[b]

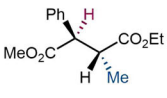

21 72% 2:1 dr

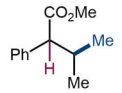

22 50%

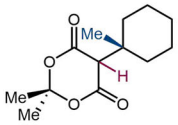

23 29% (60% brsm)

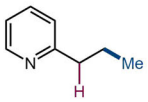

24 50% (85%)[b]

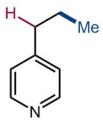

25 59% (84%)[b]

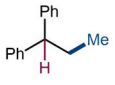

26 37%[b,c]

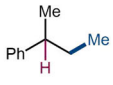

27 22%[a,c]

Carboxylic acid scope

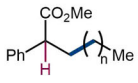

28 n = 1, 71%
29 n = 6, 69%

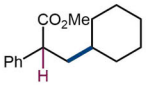

30 85%

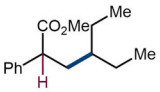

31 82%

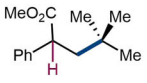

32 85%

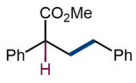

33 79%

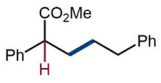

34 61%

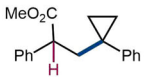

35 77%

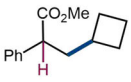

36 87%

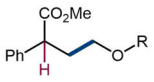

37 R = Bn, 80%
38 R = Me, 91%
39 R = Ph, 78%

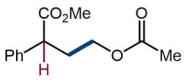

40 64%

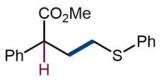

41 43%

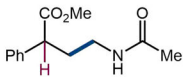

42 86%

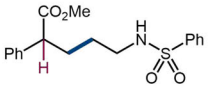

43 45%

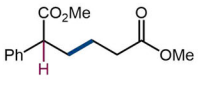

44 52%

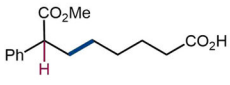

45 82%

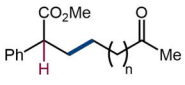

46 n = 1, 86%
47 n = 2, 75%

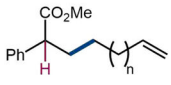

48 n = 1, 81%
49 n = 2, 79%

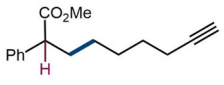

50 56%

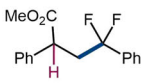

51 82%

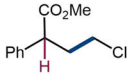

52 76%

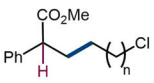

53 n = 2, 74%
54 n = 3, 87%

55 80%

56 85%

57 62%

58 70%

59 71%

60 49%

61 41%

62 87%

Reactions were conducted on 0.5 mmol scale. Yields are for isolated material following chromatography on silica gel unless otherwise noted. GC or NMR yields are reported for volatile products. [a] Yields are determined by GC analysis relative to an internal standard. [b] Yields are determined by crude ^{1}H NMR analysis relative to an internal standard. [c] HAT co-catalyst—dibenzyl disulfide (Bn_2S_2) was added (see Supporting Information).

Scheme 2. Radical trap and isotope labeling experiments.

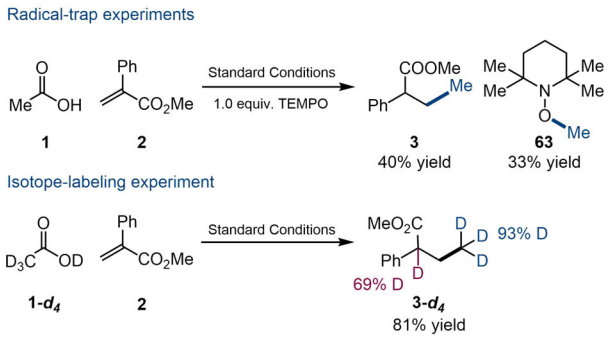

yields (**51**–**55**) with retention of the halide functionality. Also, heterocyclic substrates afforded the desired hydroalkylation products with satisfying yields (**56**–**60**) and decarboxylation of benzoylformic acid yielded the hydrobenzoylation product in moderate yield (**61**) without decarbonylation. To demonstrate the utility of this method for modifying drug targets, Gemfibrozil was alkylated (**62**) in high yield.

Scheme 2 summarizes the results of radical trap and isotope labelling experiments (see Supporting Information for experimental details). Under the standard photoreaction condition (Method B) amended with the presence of one equivalent of TEMPO (2,2,6,6-tetramethyl-1-piperidinyloxy), TEMPO–Me (**63**) was obtained in 33% yield with an attendant decrease in the yield of hydromethylation product **3**. This result is consistent with the generation of a methyl radical from the decarboxylation of acetic acid by photoexcited TiO_2. When isotope labeled d_4-acetic acid was used as substrate, 93% deuteration of the terminal methyl group and 69% deuteration at the α-position was observed in hydromethylated product **3**, indicating that the methyl group and the α-hydrogen atom indeed come from acetic acid. Notably, high isolated yields of deuterated carboxylic acids suggest the utility of the TiO_2 photoredox method in efficiently furnishing isotopically labeled targets.

The catalytic cycle shown in Figure 2 is consistent with the observed results for TiO_2 photocatalyzed hydromethylation (and alkylation) of olefins. Acetic acid adsorbs on TiO_2 anatase surface with the two oxygen atoms of the carboxylic group coordinating to neighboring titanium centers.[29] Photogenerated holes (2.7 V vs. NHE) induce C–C bond cleavage to drive the decarboxylation of surface-bonded acetate (potential of acetate: E ($AcO^{\bullet/-}$) = 2.6 V vs. NHE)[10] to afford a free methyl radical and reduced catalyst (**C**). Reduced TiO_2 is known to be blue and it is noteworthy that during photocatalysis the solution takes on a blue hue. The diffusive reflectance spectrum of TiO_2 catalyst after irradiation in the presence of acetic acid exhibits a broad absorption feature from 500 nm to 1100 nm (Figure S4), together with reduced absorbance at the band edge (<400 nm),[38] both of which are consistent with the reduced catalyst nanoparticle. Inner-sphere hole transfer from the VB of TiO_2 to the acetate facilitates the kinetics of redox-driven bond dissociation reactions.[39,40] The resulting free methyl radical is trapped by an alkene, to generate carbon-centered radical **5** at an appreciable rate constant (e.g. methyl acrylate,[41] $k = 3.4 \times 10^5$ M^{-1} s^{-1}). Electrons in the conduction band of TiO_2 (−0.5 V vs. NHE) are

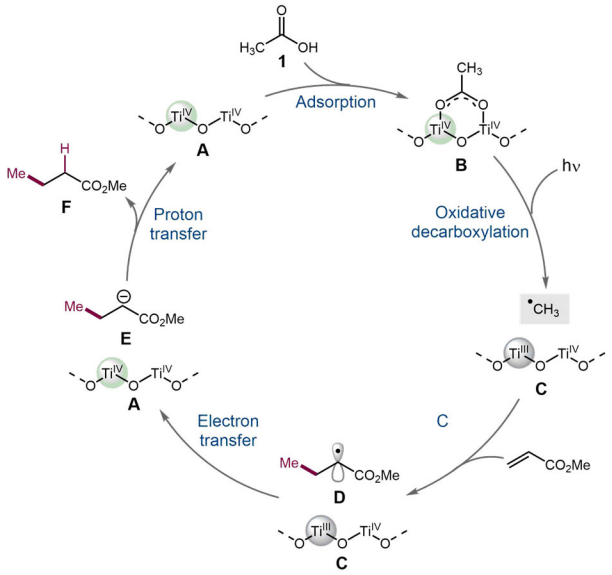

Figure 2. Catalytic mechanism for TiO_2-promoted hydromethylation of alkenes.

sufficiently reducing to drive reduction of **D** (E ($C^{\bullet}/C^{-}$) = −0.4 V vs. NHE)[42] to produce anion **E**. Proton transfer from acetic acid (pK_a = 22 in MeCN)[43] to **E** (pK_a = 40 estimated in MeCN)[44,45] closes the cycle and yields the desired hydromethylation product **F**. Alternatively, concerted proton-coupled electron transfer will also serve the purpose of reducing radical **D** to **F** (BDE = 96 kcal/mol)[46] by an electron from CB of TiO_2 and proton from acetic acid (effective BDE = 61 kcal/mol), which was determined from the following: effective BDE = 23.06 E + 1.37 pK_a + 54.9 (in MeCN).[47] Attenuation of free radical character in **D** prevents undesired dimerization and redox side reactions. Notably, the presence of both a photogenerated hole in VB and an electron in CB of TiO_2 allows for a closed and redox-neutral cycle.

Herein is described a photocatalytic hydromethylation and hydroalkylation reaction enabled by the decarboxylation of acetic acid and other simple carboxylic acids. The reaction is mediated by heterogeneous TiO_2 anatase nanoparticles with 390-nm light irradiation. A survey of the substrate scope shows that a variety of alkenes and aliphatic acids are effective coupling partners for this methodology. Compared to the more intensely explored iridium- and ruthenium-centered photoredox catalysts, the heterogeneous semiconductor TiO_2 catalyst, can access challenging intermediates such as methyl radical in a straightforward manner owing to high photoredox potentials together with a proclivity for inner-sphere redox activation. Moreover, by using the hole in the VB and the electron in the CB in concert, a closed photocatalytic cycle may be established without the need for ancillary redox partners, thus affording more simplified design strategies for photoredox methods.

ASSOCIATED CONTENT

Supporting Information

Experimental details of reaction optimization, procedures for photoreaction, mechanistic studies, independent synthesis of substares

and product characterization data. The Supporting Information is available free of charge on the ACS Publications website.

AUTHOR INFORMATION

Corresponding Author

*__Daniel G. Nocera__ – Department of Chemistry and Chemical Biology, Harvard University, 12 Oxford Street, Cambridge, Massachusetts 02138–2902, United States; orcid.org/0000-0001-5055-320X; Email: dnocera@fas.harvard.edu.

Author

__Qilei Zhu__ – Department of Chemistry and Chemical Biology, Harvard University, 12 Oxford Street, Cambridge, Massachusetts 02138–2902, United States; orcid.org/0000-0002-6360-9820.

Notes

The authors declare no competing financial interests.

ACKNOWLEDGMENT

This work was supported by the National Science Foundation under grant CHE-1855531.

REFERENCES

(1) Twilton, J.; Le, C.; Zhang, P.; Shaw, M. H.; Evans, R. W.; MacMillan, D. W. C. The merger of transition metal and photocatalysis. *Nat. Rev. Chem.* **2017**, *1*, 0052.

(2) Staveness, D.; Bosque, I.; Stephenson, C. R. J. Free radical chemistry enabled by visible light-induced electron transfer. *Acc. Chem. Res.* **2016**, *49*, 2295–2306.

(3) Romero, N. A.; Nicewicz, D. A. Organic photoredox catalysis. *Chem. Rev.* **2016**, *116*, 10075–10166.

(4) Skubi, K. L.; Blum, T. R.; Yoon, T. P. Dual catalysis strategies in photochemical synthesis. *Chem. Rev.* **2016**, *116*, 10035–10174.

(5) Chen, J.-R.; Hu, X.-Q.; Lu, L.-Q.; Xiao, W.-J. Exploration of visible-light photocatalysis in heterocycle synthesis and functionalization: Reaction design and beyond. *Acc. Chem. Res.* **2016**, *49*, 1911–1923.

(6) Tellis, J. C.; Kelly, C. B.; Primer, D. N.; Jouffroy, M.; Patel, N. R.; Molander, G. A. Single-electron transmetalation via photoredox/nickel dual catalysis: Unlocking a new paradigm for sp^3– sp^3 cross-coupling. *Acc. Chem. Res.* **2016**, *49*, 1429–1439.

(7) Zuo, Z.; Ahneman, D. T.; Chu, L.; Terrett, J. A.; Doyle, A. G.; Macmillan, D. W.C. Merging photoredox with nickel catalysis: Coupling of α-carboxyl sp^3-carbons with aryl halides. *Science*, **2014**, *345*, 437–440.

(8) Denisov, E. T.; Shestakov, A. F. Free-radical decarboxylation of carboxylic acids as a concerted abstraction and fragmentation reaction. *Kinet. Catal.* **2013**, *54*, 22–33.

(9) Hilborn, J. W.; Pincock, J. A. Rates of decarboxylation of acyloxy radicals formed in the photocleavage of substituted 1-naphthylmethyl alkanoates. *J. Am. Chem. Soc.* **1991**, *113*, 2683–2686.

(10) Kraeutler, B.; Bard, A. J. The photoassisted decarboxylation of acetate on n-type rutile electrodes—the photo-Kolbe reaction. *Nouv. J. Chim.* **1979**, *3*, 31.

(11) Eberson, L. Studies on the Kolbe electrolytic synthesis IV. A theoretical investigation of the mechanism by standard potential calculation. *Acta Chem. Scand.* **1963**, *17*, 2004–2018.

(12) Dao, H. T.; Li, C.; Michaudel, Q.; Maxwell, B. D.; Baran, P. S. Hydromethylation of unactivated olefins. *J. Am. Chem. Soc.* **2015**, *137*, 8046–8049.

(13) Cui, J.; Zhou, Q.; Pan, C.; Yabe, Y.; Burns, A. C.; Collins, M. R.; Ornelas, M. A.; Ishihara, Y. Baran, P. S. C–H methylation of heteroarenes inspired by radical SAM methyl transferase. *J. Am. Chem. Soc.* **2014**, *136*, 4853–4856.

(14) Cheng, H.; Xu, W. Recent advances in modified TiO_2 for photo-induced organic synthesis. *Org. Biomol. Chem.* **2019**, *17*, 9977–9989.

(15) Savateev, A.; Ghosh, I.; König, B.; Antonietti, M. Photoredox catalytic organic transformations using heterogeneous carbon nitrides. *Angew. Chem. Int. Ed.* **2018**, *57*, 15936–15947.

(16) Parrino, F.; Bellardita, M.; García-López, E. I.; Marcì, G.; Loddo, V.; Palmisano, L. Heterogeneous photocatalysis for selective formation of high-value-added molecules: some chemical and engineering aspects. *ACS Catal.* **2018**, *8*, 11191–11225.

(17) Kisch, H. Semiconductor photocatalysis for chemoselective radical coupling reactions. *Acc. Chem. Res.* **2017**, *50*, 1002–1010.

(18) Ghosh, I.; Khamrai, J.; Savateev, A.; Shlapakov, N.; Antonietti, M.; König, B. Organic semiconductor photocatalyst can bifunctionalize arenes and heteroarenes. *Science* **2019**, *365*, 360–366.

(19) Jiang, Y.; Wang, C.; Rogers, C. R.; Kodaimati, M. S.; Weiss, E. A. Regio- and diastereoselective intermolecular [2+2] cycloadditions photocatalyzed by quantum dots. *Nat. Chem.* **2019**, *11*, 1034–1040.

(20) Pitre, S. P.; Scaiano, J. C.; Yoon, T. P. Photocatalytic indole Diels-Alder cycloaddition mediated by heterogeneous platinum-modified titanium dioxide. *ACS Catal.* **2017**, *7*, 6440–6444.

(21) Bhat, V. T.; Duspara, P. A.; Seo, S.; Abu Bakar, N. S. B.; Greaney, M. F. Visible light promoted thiol-ene reactions using titanium dioxide. *Chem. Commun.* **2015**, *51*, 4383–4385.

(22) Kisch, H. Semiconductor photocatalysis—mechanistic and synthetic aspects. *Angew. Chem. Int. Ed.* **2013**, *52*, 812–847.

(23) Friedmann, D.; Hakki, A.; Kim, H.; Choi, W.; Bahnemann, D. Heterogeneous photocatalytic organic synthesis: state-of-the-art and future perspectives. *Green Chem.* **2016**, *18*, 5391–5411.

(24) Manley, D. W.; McBurney, R. T.; Miller, P.; Howe, R. F.; Rhydderch, S.; Walton, J. C. Unconventional titania photocatalysis: direct deployment of carboxylic acids in alkylations and annulations. *J. Am. Chem. Soc.* **2012**, *134*, 13580–13583.

(25) Manley, D. W.; McBurney, R. T.; Miller, P.; Walton, J. C.; Mills, A.; O'Rourke, C. Titania-promoted carboxylic acid alkylation of alkenes and cascade addition-cyclizations. *J. Org. Chem.* **2014**, *79*, 1386–1398.

(26) Quah, E. L.; Wilson, J. N.; Idriss, H. Photoreaction of the rutile TiO_2 (011) single-crystal surface: reaction with acetic acid. *Langmuir*, **2010**, *26*, 6411–6417.

(27) Muggli, D. S.; Keyser, S. A.; Falconer, J. L. Photocatalytic decomposition of acetic acid on TiO_2. *Catal. Lett.* **1998**, *55*, 129–132.

(28) Chen, Q.; Song, J. M.; Pan, F.; Xia, F. L.; Yuan, J. Y. The kinetics of photocatalytic degradation of aliphatic carboxylic acids in an UV/TiO_2 suspension system. *Environ. Technol.* **2009**, *30*, 1103–1109.

(29) Grinter, D. C.; Nicotra, M.; Thornton, G. Acetic acid adsorption on anatase TiO_2 (101). *J. Phys. Chem. C* **2012**, *116*, 11643–11651.

(30) Wayner, D. D. M.; Mcphee, D. J.; Griller, D. Oxidative and reductive potentials of transient free radicals. *J. Am. Chem. Soc.* **1988**, *110*, 132–137.

(31) Margrey, K. A.; Nicewicz, D. A. A general approach to catalytic alkene anti-Markovnikov hydrofunctionalization reactions via acridinium photoredox catalysis. *Acc. Chem. Res.* **2016**, *49*, 1997–2006.

(32) Miller, D. C.; Choi, G. J.; Orbe, H. S.; Knowles, R. R. Catalytic olefin hydroamidation enabled by proton-coupled electron transfer. *J. Am. Chem. Soc.* **2015**, *137*, 13492–13495.

(33) Ruccolo, S.; Qin, Y.; Schnedermann, C.; Nocera, D. G. General strategy for improving the quantum efficiency of photoredox hydroamidation catalysis. *J. Am. Chem. Soc.* **2018**, *140*, 14926–14937.

(34) Devery, J. J., III; Douglas, J. J.; Nguyen, J. D.; Cole, K. P.; Flowers, R. A., II; Stephenson, C. R. J. Ligand functionalization as a

deactivation pathway in a *fac*-Ir(ppy)$_3$-mediated radical addition. *Chem. Sci.* **2015**, *6*, 537–541.

(35) O'Brien, C. J.; Droege, D. G.; Jiu, A. Y.; Gandhi, S. S.; Paras, N. A.; Olson, S. H.; Conrad, J. Photoredox cyanomethylation of indoles: Catalyst modification and mechanism. *J. Org. Chem.* **2018**, *83*, 8926–8935.

(36) (a) Dewar, M. J. S.; Olivella, S. Ground states of molecules. 48. MINDO/3 study of some radical addition reactions. *J. Am. Chem. Soc.* **1978**, *100*, 5290–5295.

(37) Beckwith, A. L. J.; Schiesser, C. H. Regio- and stereoselectivity of alkenyl radical ring closure: A theoretical study. *Tetrahedron* **1985**, *41*, 3925–3941.

(38) Schrauben, J. N.; Hayoun, R.; Valdez, C. N.; Braten, M.; Fridley, L.; Mayer, J. M. Titanium and zinc oxide nanoparticles are proton-coupled electron transfer agents. *Science* **2012**, *336*, 1298–1301.

(39) Savéant, J. M. Dissociative electron transfer. New tests of the theory in the electrochemical and homogeneous reduction of alkyl halides. *J. Am. Chem. Soc.* **1992**, *114*, 10595–10602.

(40) Houmam, A. Electron transfer initiated reactions: Bond formation and bond dissociation. *Chem. Rev.* **2008**, *108*, 2180–2237.

(41) Fischer, H.; Radom, L. Factors controlling the addition of carbon-centered radicals to alkenes—an experimental and theoretical perspective. *Angew. Chem. Int. Ed.* **2001**, *40*, 1340–1371.

(42) Bortolamei, N.; Isse, A. A.; Gennaro, A. Estimation of standard reduction potentials of alkyl radicals involved in atom transfer radical polymerization. *Electrochim. Acta.* **2010**, *55*, 8312–8318.

(43) Kolthoff, I. M.; Chantooni, M. K. Jr.; Bhowmik, S. Dissociation constants of uncharged and monovalent cation acids in dimethyl sulfoxide. *J. Am. Chem. Soc.* **1968**, *90*, 23–28.

(44) Zhang, X.-M.; Bordwell, F. G.; Van der Puy, M.; Fried, H. E. Equilibrium acidities and homolytic bond dissociation energies of the acidic carbon-hydrogen bonds in N-substituted trimethylammonium and pyridinium cations. *J. Org. Chem.* **1993**, *58*, 3060–3066.

(45)Ding, F.; Smith, J. M.; Wang, H. First-principle calculation of pK_a values for organic acids in nonaqueous solution. *J. Org. Chem.* **2009**, *74*, 2679–2691.

(46) Brocks, J. J.; Beckhaus, H.-D.; Beckwith, A. L. J.; Rüchardt, C. Estimation of bond dissociation energies and radical stabilization energies by ESR spectroscopy. *J. Org. Chem.* **1998**, *63*, 1935–1943.

(47) Calculated from equation: effective BDFE = 23.06 E + 1.37 pK_a + 54.9 (in MeCN). See: Warren, J. J.; Tronic, T. A.; Mayer, J. M. Thermochemistry of proton-coupled electron transfer reagents and its implications. *Chem. Rev.* **2010**, *110*, 6961–7001.